Ennis, H. L., & Sussman, M. (1975) *J. Bacteriol. 124*, 62–64.
Giorda, R., & Ennis, H. L. (1987) *Mol. Cell. Biol. 6*, 2097–2103.
Henikoff, S. (1984) *Gene 28*, 351–359.
Kelly, L. J., Kelly, R., & Ennis, H. L. (1983) *Mol. Cell. Biol. 3*, 1943–1948.
Lee, H., Simon, J. A., & Lis, J. T. (1988) *Mol. Cell. Biol. 8*, 4727–4735.
Lund, P. K., Moats-Staats, B. M., Simmons, J. G., Hoyt, E., D'Ercole, A. J., Martin, F., & Van Wyk, J. J. (1985) *J. Biol. Chem. 260*, 7609–7613.
Maniatis, T., Fritsch, E. F., & Sambrook, J. (1982) *Molecular Cloning: A Laboratory Manual*, Cold Spring Harbor Laboratory, Cold Spring Harbor, NY.
Miller, J., McLachlan, A. D., & Klug, A. (1985) *EMBO J. 4*, 1609–1614.
Müller-Taubenberger, A., Westphal, A., Jaeger, E., Noegel, A., & Gerisch, G. (1988a) *FEBS Lett. 229*, 273–278.
Müller-Taubenberger, A., Hagmann, J., Noegel, A., & Gerisch, G. (1988b) *J. Cell. Sci. 90*, 51–58.
Özkaynak, E., Finley, D., & Varshavsky, A. (1984) *Nature (London) 312*, 663–666.
Redman, K. L., & Rechsteiner, M. (1988) *J. Biol. Chem. 263*, 4926–4931.
Sanger, F., Nicklen, N., & Coulson, A. R. (1977) *Proc. Natl. Acad. Sci. U.S.A. 74*, 5463–5467.
Schlesinger, D. H., Goldstein, G., & Niall, H. D. (1975) *Biochemistry 14*, 2214–2218.
Sharp, P. M. & Li, W.-H. (1987) *Trends Ecol. Evol. 2*, 328–332.
St. John, T., Gallatin, W. M., Siegelman, M., Smith, H. T., Fried, V. A., & Weissman, I. L. (1986) *Science 231*, 845–850.
Sussman, M., & Brackenbury, R. (1976) *Annu. Rev. Plant Physiol. 27*, 229–265.
Sussman, R., & Sussman, M. (1967) *Biochem. Biophys. Res. Commun. 29*, 53–55.
Vierstra, R. D., Langan, S. M., & Schaller, G. E. (1986) *Biochemistry 25*, 3105–3108.
Vincent, A. (1986) *Nucleic Acids Res. 14*, 4385–4391.
Westphal, M., Müller-Taubenberger, A., Noegel, A., & Gerisch, G. (1986) *FEBS Lett. 209*, 92–96.
Wiborg, O., Pedersen, M. S., Wird, A., Berglund, L. E., Marker, K. A., & Vuust, J. (1985) *EMBO J. 4*, 755–759.

Binding of Actinomycin D to $[d(ATCGAT)]_2$: NMR Evidence of Multiple Complexes†

Ning Zhou,‡ Thomas L. James, and Richard H. Shafer*
Department of Pharmaceutical Chemistry, School of Pharmacy, University of California, San Francisco, California 94143
Received November 3, 1988; Revised Manuscript Received March 3, 1989

ABSTRACT: Actinomycin D (actD) binds to the oligonucleotide $[d(ATCGAT)]_2$ with a hypochromatic and red-shifted visible absorbance band compared to free drug and a CD spectrum with double negative bands at 460 and 385 nm. These spectral features are similar to those of the actD–$[d(ATGCAT)]_2$ complex, while actD–$[d(AT)_5]_2$ gives spectra similar to those of free drug. Upon dilution or raising the temperature, the spectral characteristics accompanying complex formation disappear in the actD–$[(ATCGAT)]_2$ sample but remain in the actD–$[d(ATGCAT)]_2$ complex under the same experimental conditions. These results suggest that (a) sequence-specific binding of actD occurs with $[d(ATCGAT)]_2$ but not with $[d(AT)_5]_2$, (b) the binding is not as strong as with $[d(ATGCAT)]_2$, and (c) actD binds $[d(ATCGAT)]_2$ with the same mechanism as it binds $[d(ATGCAT)]_2$, i.e., by intercalation. From NMR spectra of the actD–$[d(ATCGAT)]_2$ complex, three types of signals can be detected below 20 °C, one major and two minor ones. At higher temperatures, exchange between the two minor ones becomes fast enough that only one type of minor signal was seen. Partial resonance assignments were made by using 2D nuclear Overhauser effect (NOE) and 2D homonuclear Hartmann–Hahn (HOHAHA) experiments. Proton chemical shift changes of the major complex are consistent with actD chromophore ring intercalation between hexamer base pairs. Data from NOE-detected dipolar interactions between actD and $[d(ATCGAT)]_2$ protons were interpreted in terms of a major complex with the actD chromophore ring system intercalated at the CG position and minor complexes with the drug intercalated off center at the GA positions. While the centrally intercalated complex still exists at a 1:2 $[d(ATCGAT)]_2$:actD ratio, there is also evidence for a complex consisting of two bound actD molecules per duplex.

Actinomycin D (actD) (Figure 1) is currently used as an antitumor drug in routine clinical treatment of a limited number of cancers. Its binding to DNA has been extensively studied [see review by Waring (1981)]. A widely accepted model of the actD–DNA complex is one with the drug chromophore intercalated between 5′-GpC-3′ and its peptide side chains lying in the minor groove. This model complex is stabilized by a strong hydrogen bond between G NH_2 and Thr C=O, a weak hydrogen bond between G N3 and Thr αH, and stacking forces between the actD chromophore ring and the G base ring, as well as by numerous hydrophobic interactions between the drug peptide chains and DNA minor groove

† This work was supported by USPHS Grant CA 27343 awarded by the National Cancer Institute, DHHS.
* Address correspondence to this author.
‡ Present address: Department of Biological Sciences, University of Calgary, AB T2N IN4, Canada.

0006-2960/89/0428-5231$01.50/0

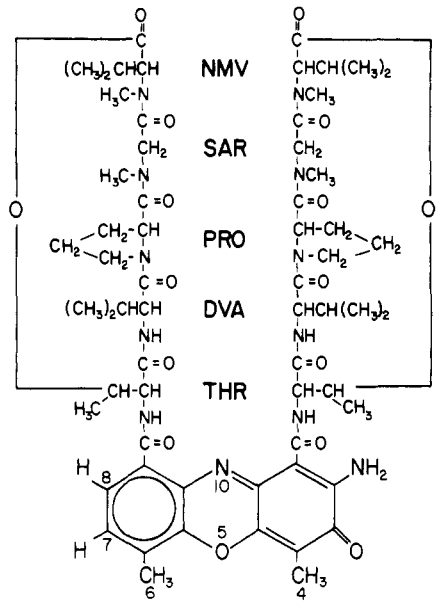

FIGURE 1: Chemical structure of actinomycin D.

surface atoms. A strong binding specificity for 5′-GC-3′ was found for the actD–DNA interaction, which has been attributed (Sobell, 1973; Remers, 1979) to the correct geometry for formation of the two hydrogen bonds between actD and the G residue when the actD ring is situated at the 3′ side of the G residue. Other binding studies demonstrated that poly[d(GT)]·poly[d(AC)] binds actD approximately one-fifth as well as poly[d(GC)], and significant actD binding was detected with poly[d(TAC)]·poly[d(GTA)] but not with poly[d(ATC)]·poly[d(GAT)] (Wells & Larson, 1971). Allen et al. (1976, 1977) reported that GC as well as CG were good binding sites for actD based on first-neighbor analysis of CD spectra of poly[d(GC)]. A theoretical study (Lybrand et al., 1986) suggested that CG is not a better actD binding site than AT or TA due to distorted hydrogen-binding geometry.

Studies of actD–oligonucleotide sequence-specific interactions to date have involved dinucleotides (Krugh, 1972; Schara & Müller, 1972) and oligonucleotides containing GC sequences (Reid et al., 1983; Brown et al., 1984) or coexisting CG and GC sequences (Wilson et al., 1986; Scott et al., 1988). The actD binding behavior of CG sites of oligonucleotides in the absence of the strong binding site GC has not been studied experimentally. The oligonucleotide $[d(ATCGAT)]_2$ provides such a case, along with the possibility of analyzing different potential binding sites, e.g., CG vs GA. It also presents an opportunity to examine the so-called neighbor exclusion effect when the binding properties of adjacent sites are similar.

The biological activity of actD has been related to its association and dissociation properties with DNA (Müller & Crothers, 1968). Studies on actD interaction with DNA sequences other than GC will give information about structural requirements for actD intercalation, information about how actD differentiates its preferred site (GC) from other sites, and information useful for understanding of the overall picture of the actD–DNA interaction as well.

In this work we report visible and CD spectral evidence for binding of actD with $[d(ATCGAT)]_2$ by intercalation; 1D and 2D proton NMR experiments were used to determine further the types of complexes formed and to define intercalating sites.

Materials and Methods

ActD was purchased from Calbiochem, and the hexanucleotide pentaphosphate 5′-d(ATCGAT)-3′ was purchased from Pharmacia. These were used without further purification. The 5′-d(ATGCAT)-3′ was a gift from Dr. C. Levenson, Cetus Corp., and was synthesized by standard triester techniques (Narang et al., 1980); its purity was checked by HPLC, base composition analysis, ^1H NMR, and ^{31}P NMR. The 5′-d-$(AT)_5$-3′ oligonucleotide was obtained from Dr. G. Zon, Applied Biosystems, inc. Solvent D_2O was purchased from ICN Biochemicals, Inc. Buffer reagents were from Sigma. Concentrations were determined spectrophotometrically, using ϵ_{260} = 79 500 for d(ATCGAT) (per mole of duplex measured in buffer containing 1 M NaCl) and ϵ_{440} = 24 450 for actD.

Visible absorbance spectra were determined on a Gilford 2600 spectrometer, and CD spectra were measured by using a Jasco J-500 spectropolarimeter.

The d(ATCGAT) samples for NMR measurements were made in aqueous phosphate buffer solution (100 mM phosphate, pH 7; 180 mM NaCl, 0.2 mM EGTA). The concentration of d(ATCGAT) was 8 mM (strand concentration) in all cases except in 1:2 and 1:3 hexamer–drug samples, which were 4 mM in strand concentration. A 4 mM stock solution of actD in H_2O was made, and aliquots were added either to a 90% H_2O/10% D_2O mixture or pure D_2O. Various amounts of lyophilized d(ATCGAT) were redissolved in this to make different drug–hexamer mixtures.

NMR experiments were carried out on a 500-MHz (GE GN-500) spectrometer equipped with an Oxford Instruments magnet and a Nicolet 1280 computer. Two-dimensional (2D) experimental data were processed on a Vax 11/750 computer (Digital Equipment Corp.) using software developed by Drs. S. Manogaran and R. Scheek at University of California, San Francisco.

One-dimensional (1D) spectra in 90% H_2O/10% D_2O buffer solution were obtained by using the $1\bar{3}3\bar{1}$ solvent suppression sequence (Hore, 1983) with the carrier frequency set at the water resonance and the interval delay set at 125 μs, so that the center of excitation was at the imino proton resonance region. 1D truncated driven NOE difference spectra were obtained from experimental data sets with 600 ms of preirradiation alternately placed on the imino proton resonances and off resonance. A delay of 1 ms between preirradiation and the exciting pulse was used along with a repetition time of 4 s.

2D NOE spectra were acquired in the pure absorption mode by using the method of States et al. (1982). The exciting 90° pulse in the 2D NOE experiments was replaced by a $1\bar{3}3\bar{1}$ pulse, and a short homospoil pulse was applied at the beginning of the mixing time to suppress the solvent peak for samples in 90% H_2O/10% D_2O buffer (Boelens et al., 1985). Mixing times were varied from 100 to 400 ms. Proton scalar connectivities were determined by 2D homonuclear Hartmann–Hahn relayed spectroscopy (HOHAHA; Davis & Bax, 1985). 1D imino proton NOEs were measured at 12 °C; 2D NOE experiments were carried out at 15 and 20 °C. Chemical shifts were reported at 15 °C. The COSY and HOHAHA experiments were acquired at 20 °C to obtain better results on the major complex resonances. 2D experiments in D_2O consisted of 4K data points stored in alternating blocks with 32 scans each at 400 t_1 values. The free induction decays were modified via shifted sine bell apodization and exponential multiplication in the t_2 dimension and by shifted sine bell multiplication in the t_1 dimension with zero filling in the t_1 dimension prior to Fourier transformation. The processing resulted in a final data set of 1k × 1k size. Pulse repetition time was 4 s. The carrier was set at the HDO signal, and the spectral width was 5000 Hz. 2D experiments in 90% H_2O/10% D_2O had a spectral

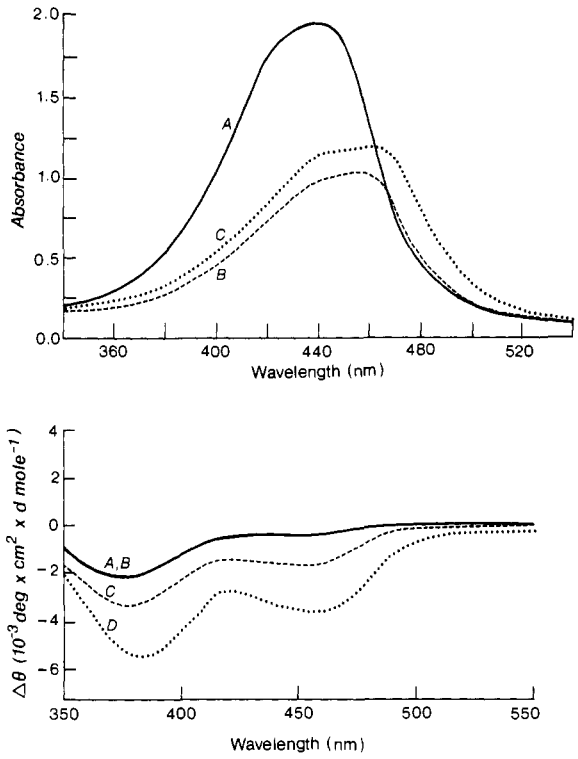

FIGURE 2: (Top) Absorption spectra of free actD (A), actD in the presence of [d(ATCGAT)] (B), and [d(ATGCAT)] (C) at 20 °C. The concentration of free actD was 0.08 mM; concentrations of actD–DNA mixture samples were 0.08 mM actD and 0.24 mM oligonucleotide strand in 100 mM phosphate buffer solution (pH 7) with 180 mM NaCl. (Bottom) Circular dichroism spectra at 20 °C of free actinomycin D (A) and actinomycin D in the presence of $d(AT)_5$ (B), d(ATCGAT) (C), and d(ATGCAT) (D), in 100 mM phosphate buffer solution (pH 7) with 180 mM NaCl. The concentration of actD was 0.02 mM; concentration of oligonucleotide was 0.04 mM in strand. One-centimeter length cell was used.

width of 10000 Hz. Some of these were collected in 8K data points, so comparable resolution was obtained with a final data set size of 2k × 1k. A polynomial base-line correction procedure along the t_2 dimension of the Fourier-transformed data set was performed.

Results and Discussion

Visible Absorbance and CD Spectra. Figure 2 (top) shows the 340–520-nm region absorbance spectra of actD (A) and 1:1 mixtures of actD–$[d(ATCGAT)]_2$ (B) and actD–$[d(ATGCAT)]_2$ (C). Curve C has a red-shifted band with reduced absorbance compared to curve A; this is considered to be the result of the actD chromophore ring system intercalating between the central GC base pairs of $[d(ATGCAT)]_2$. Curve B shows further reduced absorbance intensity with a similar red shift and shape as curve C, suggesting that intercalation of the actD ring system also occurs with $[d(ATCGAT)]_2$. The absorbance spectrum of the actD–$[d(AT)_5]_2$ 1:1 mixture (not shown) had a spectrum similar to that of free actD with a peak at 440 nm but slightly reduced intensity. When the sample concentrations were reduced by a factor of 4, the actD–$[d(ATGCAT)]_2$ mixture still gave an absorbance spectrum similar to that at higher concentration, Figure 2 (top), curve C, while the actD–$[d(ATCGAT)]_2$ mixture possessed a spectrum very similar to that of actD alone.

Plotted in Figure 2 (bottom) are CD spectra of these low-concentration samples. In the presence of $[d(ATCGAT)]_2$ (C), the characteristics of actD–$[d(ATGCAT)]_2$ (curve D) with two negative minima at 460 and 385 nm were retained. However, the amplitude was reduced to 40% at 460 nm and 38% at 385 nm compared to that of actD–$[d(ATGCAT)]_2$ (both relative to actD alone, curve A). In the presence of $[d(AT)_5]_2$ (B), only very small changes occurred. These observations are consistent with the notion that actD binds to $[d(ATCGAT)]_2$ by intercalation; however, the binding is not as strong as with $[d(ATGCAT)]_2$.

In addition to the lower stability manifested upon dilution, the actD–$[d(ATCGAT)]_2$ binding was also less stable than the actD–$[d(ATGCAT)]_2$ complex at higher temperatures. The actD–$[d(ATGCAT)]_2$ sample gave similar spectra at 4, 15, and 20 °C, but decreased slightly in intensity at both 385 and 460 nm when the temperature was increased to 32 °C (data not shown). For the actD–$[d(ATCGAT)]_2$ sample, the CD spectra also did not change much within the temperature range 4–20 °C, but the intensities of these two negative bands were reduced significantly at 32 °C. As will be shown in the next section, NMR measurements reveal the formation of more than one type of actD–$[d(ATCGAT)]_2$ complex with relative populations varying with temperature in the range 4–20 °C. The lack of temperature dependence in the CD spectra in this range suggests that the different complexes share an intercalative binding mechanism.

A recent absorbance study by Chen (1988) indicated reduced binding of actD to d(TATACGTATA) compared to actD–d(ATATGCATAT) binding. These observations were consistent with our absorbance spectral results for actD binding to the two hexamers.

NMR Measurements. The nomenclature used for the residues in $[d(ATCGAT)]_2$ is

5'- A1 · T2 · C3 · G4 · A5 · T6 - 3'

3' - T12 · A11 · G10 · C9 · T8 · A7 - 5'

Standard IUPAC numbering for atoms is used. The structure of actD with numbering of the chromophore ring protons is shown in Figure 1.

Hexamer Imino and Amino Protons. Assignment of free $[d(ATCGAT)]_2$ imino proton resonances can be made from their differential broadening behavior with increasing temperature change, and they are labeled in the spectra in Figure 3. Upon addition of 0.3 equiv of actD to the hexamer, two new imino proton peaks appeared upfield at 12.45 and 12.10 ppm. There were also new peaks at 13.83 ppm and at about 12.75 ppm (Figure 3). The major new peak at 12.10 ppm and that at 12.45 ppm increase in intensity, maintaining the same relative ratio (about 7:1) up to 1:1 actD–$d(ATCGAT)_2$. As additional amounts of drug are added, the peak at 12.45 ppm decreases in intensity and becomes very small in the 3:1 drug–hexamer sample. The 3:1 sample imino region spectrum was very similar to that of the 2:1 sample, except that the peaks at 12.45 and 13.37 ppm were lower in intensity. NOE measurements and temperature studies established the assignments as follows. The most upfield signal (12.10 ppm) was resolved into two peaks of essentially equal intensity by resolution enhancement and was assigned to the G4/G10 NH protons (Figure 4) on the basis of 2D NOE cross-peaks with C3 NH_2^d and C9 NH_2^d and with C3 NH_2^u and C9 NH_2^u (superscripts d and u denote downfield and upfield NH_2 proton peaks, respectively). These dipolar connectivities were also detected in 1D NOE experiments. Each pair of cytosine NH_2 protons is characterized by a 2D NOE cross-peak between NH_2^u and NH_2^d; they also form part of a proton relaxation network exhibiting NOE cross-peaks to the C H5 proton (Figure 4). Assignment of the upfield component of the 12.10 ppm peak

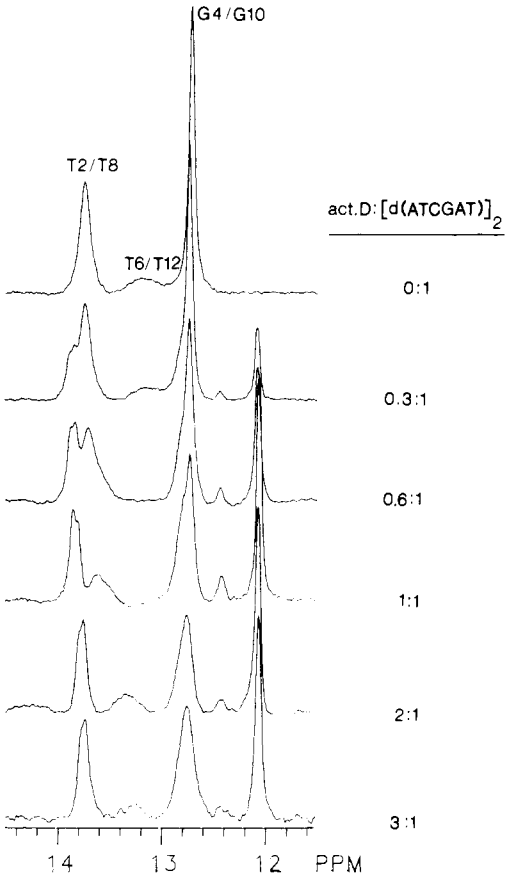

FIGURE 3: Imino proton region from the spectra of actD–[d-(ATCGAT)]$_2$ mixtures at various drug:DNA ratios as indicated in the plot. The spectra were obtained with 90% H_2O/10% D_2O phosphate buffer solution at 15 °C by using the 1$\bar{3}$3$\bar{1}$ solvent suppression sequence (Hore, 1983).

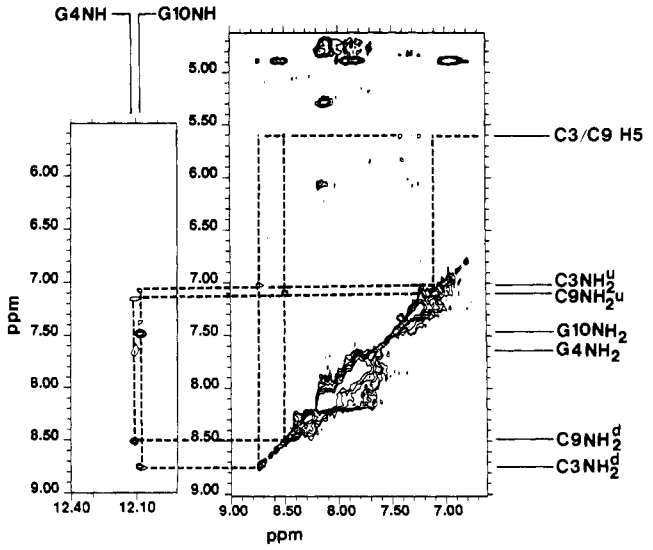

FIGURE 4: 2D NOE contour plots of 1:1 actD–[d(ATCGAT)]$_2$ (4 mM) at 15 °C in 90% H_2O/10% D_2O phosphate buffer solution (100 mM phosphate, 180 mM NaCl, 0.02 mM EGTA, pH 7). A mixing time of 150 ms was used. The assignment of the major complex G and C imino and amino protons is indicated, along with the C H5 protons. Note that the *x*-axis scale is different in upfield and downfield regions, so that NOE cross-peaks from the major G4 NH and G10 NH signals can be clearly distinguished. See Materials and Methods for other experimental details.

to G10 NH and the downfield one to G4 NH (see Figure 4) was made arbitrarily. (Note the symmetry in the hexamer itself permits this arbitrary assignment.) On the basis of this assignment, it was then possible to assign the C3 NH_2 and C9

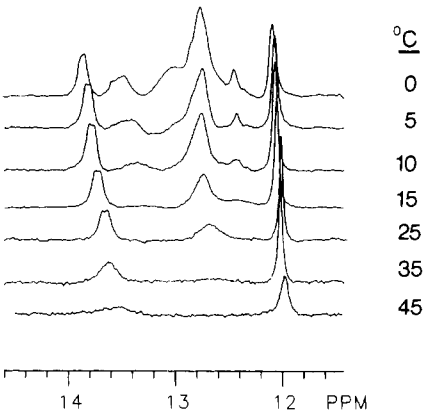

FIGURE 5: Imino proton spectra of 2:1 actD–[d(ATCGAT)]$_2$ duplex (4 mM drug and 2 mM DNA spectra in phosphate buffer with 180 mM NaCl, 0.2 mM EGTA, pH 7, in 90% H_2O/10% D_2O) at different temperatures as indicated. The 1$\bar{3}$3$\bar{1}$ solvent suppression sequence was used (Hore, 1983).

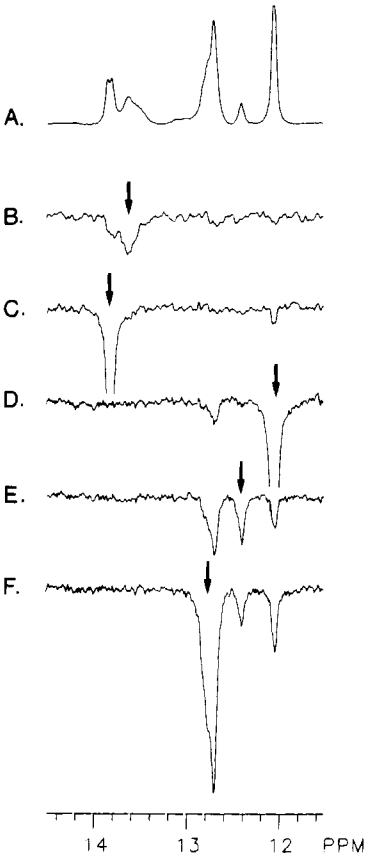

FIGURE 6: Truncated driven NOE difference spectra of imino proton region for 1:1 actD–[d(ATCGAT)]$_2$ sample. The preirradiation time was 600 ms, and the temperature was 12 °C; see Materials and Methods for further details. The spectrum with off-resonance preirradiation is (A), and (B)–(F) result from preirradiation at frequencies indicated by arrows.

NH_2 protons by reference to the observed NOE contacts between imino and amino protons within one base pair. Thus, the C3 NH_2 protons showed NOEs to the G10 NH proton, and the C9 NH_2 protons showed NOEs to the G4 NH proton, as illustrated in Figure 4. Furthermore, the C3 and C9 NH_2^d protons also give rise to NOEs to the C3/C9 H5 at 5.61 ppm (see below). Only the C9 NH_2^u–C9 H5 cross-peak was detected, not the C3 NH_2^u–C3 H5 one. The G4/G10 NH peak at 12.10 ppm was the most stable imino signal with increasing temperature at both 1:1 and 2:1 (Figure 5) actD:[dATCGAT)]$_2$ ratios.

The two signals at 12.45 and 12.75 ppm were also assigned to G4/G10 NH protons on the basis of saturation-transfer experiments. At 12 °C, the exchange rates between these two signals and the 12.10 ppm G4/G10 NH signal are sufficient that saturation transfer was observed (Figure 6D–F). Saturation transfer and/or NOE was also observed between these two minor signals. The 12.75 ppm signal is close to the free hexamer G4/G10 NH resonance; similar saturation-transfer results were obtained in the actD–$[d(ATCGAT)]_2$ 2:1 sample. Hence, these are not due to residual free hexamer signal.

As mentioned above, two pairs of C3 and C9 NH_2 signals of the major complex were identified. The downfield one in each pair gave a stronger NOE cross-peak to the major G NH signal than to the upfield one (Figure 4) and was assigned to the amino proton involved in Watson–Crick hydrogen bonding. Two signals at 7.63 and 7.49 ppm also gave NOE cross-peaks to the major complex G4 NH, G10 NH protons (Figure 4) and were thus assigned to be G4 NH_2 and G10 NH_2 protons, respectively, of the major complex. It is interesting to note that these G amino protons did not give cross-peaks to the water signal at 15 °C and a mixing time of 150 ms, while for DNA oligomers alone, G amino proton–water exchange peaks are usually detected under similar conditions (Boelens et al., 1985; D. Kerwood and T. L. James, unpublished results). This suggests that in the actD–$[d(ATCGAT)]_2$ complex the G NH_2 protons become less accessible to solvent and is consistent with the drug molecule situated in the minor grooven of the hexamer, burying the G NH_2 protons inside.

Next the downfield imino signals (13.83, 13.80 ppm) were assigned to T2/T8 NH in the major complex from the NOE difference peak with G4/G10 NH at 12.10 ppm (Figure 6C); a reversed NOE to these signals while G4/G10 NH was irradiated was not detected (Figure 6D). These T2/T8 NH signals are further coupled to two protons in the aromatic region: 13.83 to 7.99 ppm and 13.80 to 7.93 ppm. The aromatic protons were thus assigned to A5/A11 H2 in the major complex. It was not possible to distinguish between T2 NH and T8 NH or between A5 and A11 H2 protons.

The T6/T12 imino proton signal observed with the free hexamer became too small to detect in the 0.6:1 drug–duplex sample, as illustrated in Figure 3. Observation of these protons in the bound complexes was difficult. In the spectra of Figure 3 at 15 °C, there is little evidence of these signals, although there is a small but definite signal at the 2:1 stoichiometry at 13.3 ppm that cannot arise from free hexamer. Whether this is from a terminal or internal AT base pair is not clear. Figure 5 displays imino proton spectra at lower temperatures for the 2:1 drug–duplex sample. Here one can see considerably more peaks at temperatures below 15 °C. For example, at 0 °C there is a broad signal at 13.5 ppm as well as a broad shoulder at 13 ppm on the large peak at 12.75 ppm. Furthermore, the peak at 12.75 appears to have a very slight additional shoulder just upfield of the broad shoulder. Again, it is difficult to assign these resonances to particular imino protons, although it is likely that some of them represent terminal imino protons of bound complexes.

Examination of the spectral changes over a temperature range from 0 to 45 °C reveals several features (Figure 5). First, at temperatures above 20 °C, only three imino proton peaks can be seen. As the temperature is lowered, additional peaks emerge, as discussed above, with increasing amplitude. This behavior was also observed for nonexchangeable protons. Second, as the temperature is raised above 20 °C, the three peaks broaden and disappear sequentially. The first peak to disappear, at 35 °C, is the one at 12.75 ppm. This peak has

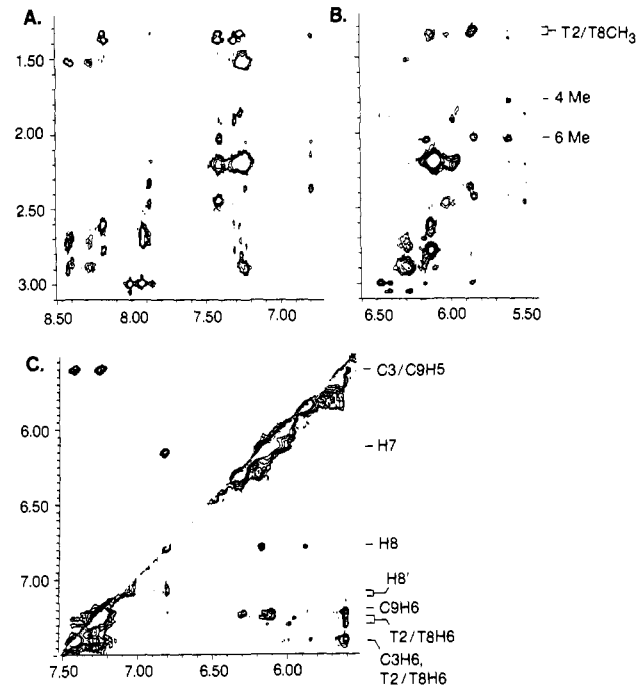

FIGURE 7: Expanded regions of NOESY contour plot, with a HOHAHA experiment contour plot replacing the upper left triangle of part C. In the proton labels, a prime indicates those from the minor drug–hexamer complex(es).

been assigned to the G4/G10 protons of one of the minor complexes, observed in the 1:1 drug–duplex sample, and probably belongs to a complex containing two bound actD molecules. The second peak that disappears is the downfield one assigned to the T2/T8 imino proton of the major complex. Finally, the most upfield peak, assigned to the G4/G10 proton of the major complex, persists to the highest temperature. These results indicate that the major complex is the most thermally stable complex with regard to exchange of imino protons with solvent. This may imply either that this complex is the most stable thermodynamically or that the DNA conformation in this complex provides the maximum protection from solvent. This latter explanation is consistent with a distortion of the helix at the central GC base pairs in the complex containing two bound drug molecules at the GA sites.

Nonexchangeable Resonance Assignments. Due to formation of multiple complexes and exchange effects, complete systematic assignment of resonances was not feasible. 2D HOHAHA and NOE experiments led to partial assignments for the major complex in the 1:1 sample at 15 °C, which are summarized in Table I together with imino and amino proton assignments discussed above. Free hexamer signals were undetectable at 1:1 stoichiometry.

The spin systems of the drug side-chain amino acids NMV, D-Val, and Thr and part of Pro were identified from HOHAHA experiments. The drug chromophore ring protons from the major complex were assigned from the HOHAHA connectivity between 7H and 8H (Figure 7) and from strong NOE contacts between 7H and 6 CH_3, between 7H and 8H (Figure 7), and between 6 CH_3 and 4 CH_3 (data not shown). Another 8H signal was identified and related to the major complex 8H signal by cross-peaks in the 2D NOE experiment at 15 °C. Weak cross-peaks connected the major 8H signal (6.80 ppm) to signals at 7.10 and 7.05 ppm (Figure 7); at 20 °C, the 7.10 and 7.05 ppm signals merged into one signal, which produced a stronger cross-peak with the major 8H signal. This is characteristic of cross-peaks resulting from chemical exchange. The two minor 8H peaks probably arise from two different

Table I: Proton Chemical Shifts of actD–[d(ATCGAT)]$_2$ Major Complex[a]

(A) Hexamer Protons

	A1/A7		T2/T8		C3/C9		G4/G10		A5/A11		T6/T12	
	b	*c*	*b*	*c*	*b*	*c*	*b*	*c*	*b*	*c*	*b*	*c*
H8(6)	8.16	8.19	7.39	7.28	7.47	7.42	7.90	7.93	8.20	8.44	7.14	7.23
		8.18•		7.32•		7.23				8.42◆		7.27◆
H5(2) or CH_3	7.82	7.85	1.27	1.35	5.59	5.61			7.91	7.99	1.36	1.49
				1.31•						7.93		1.52◆
H1′	6.11	6.14	6.03	5.99	5.62	5.84	5.64	5.49	6.27	6.28	6.07	6.12
				5.94						6.18		6.10
H2″	2.85	2.78	2.49	2.20	2.40	2.44	2.79	2.72	2.91	2.90	2.18	2.17
				2.18						2.86		
H2′	2.68	2.61	2.16	1.89	2.03	2.17	2.71	2.67	2.67	2.74	2.18	2.17
				1.84						2.69		
H3′	4.83	4.83	4.88	4.83	4.86	5.00	5.03	4.77	5.00	5.07	4.54	4.54
										5.04		4.53
H4′	4.22	4.23	4.26	4.10	4.14	4.12	4.37	4.10	4.46	4.45	4.00	4.02
												3.99
H5′H5″	3.79	3.79	4.15		4.12		4.13		4.25	4.29	4.31	4.08
							4.04			4.13		4.11
NH			13.78	13.83			12.79	12.10		13.25	12.75	
				13.80								
NH_2[d]					8.48	8.49*		7.49*				
						8.75		7.63				
NH_2[u]					6.87	7.10*						
						7.04						

(B) Drug Protons

	H8	H7	$6CH_3$	$4CH_3$	
chromophore	6.80	6.17	2.05	1.78	
	α	*β*	*γ*	*δ*	NCH_3
Thr	4.77	5.16	1.34		
	4.59	5.14	1.31		
D-Val	3.62	2.14	1.05 0.85		
	3.57	2.13	1.05 0.85		
Pro	6.48	2.51	2.83	3.64	
	6.42				
NMV	2.94	2.48	0.94 0.82		2.97

[a] Chemical shifts are relative to sodium 3-(trimethylsilyl)[2,2,3,3-D_4]propionate, at 15 °C. Signals marked with a dot, a diamond, and an asterisk are from the same strand; correlations between these segments were not achieved. [b] This column is free [d(ATCGAT)]$_2$ proton chemical shifts. [c] Chemical shifts of hexamer in 1:1 actD–[d(ATCGAT)]$_2$ major complex.

orientations of the actD chromophore ring with respect to the hexamer. These two orientations most likely involve intercalation at the off-center GA site (vide infra). When temperature increases, the "flip" of the actD ring between these two orientations becomes faster and causes peaks to merge. From the observed peak coalescence, the average lifetime of the off-center complexes is estimated to be $\sim 10^{-2}$ s. The total intensity of the two minor 8H peaks is about half that of the major 8H peak at 15 °C. Only one major complex 8H signal was observed, suggesting that the drug chromophore in the major complex is situated at the central CG position. The minor H7 peaks were not observed, possibly due to overlap with the major H7 or other peak.

The A5/A11 H2 signals were assigned as discussed above. A partially relaxed inversion-recovery experiment revealed three slowly relaxing signals at 7.99, 7.93, and 7.85 ppm, with the 7.85 ppm signal having larger (negative) intensity. This 7.85 ppm signal was assigned to A1/A7 H2. This assignment was further supported by its NOE contact to A1/A7 H1′ protons at 6.14 ppm (assigned from intraresidue hexamer NOE contacts) with a weak cross-peak. The C3/C9 H5 scalar connectivity to C3 H6 and C9 H6 is established by HOHAHA peaks (Figure 7); from the assigned C3/C9 H5 signal (5.61 ppm) (see above section), two C H6 signals were identified at 7.42 and 7.23 ppm with two equally strong cross-peaks. Since the minor complex 7H–8H connectivity was too weak to give a detectable HOHAHA cross-peak, these two C H6 signals were both assigned to the major complex. This implies a loss of duplex symmetry in the drug complex for the C H6 protons, also seen with the G NH imino proton. The peak at 5.88 ppm was tentatively assigned to C3/C9 H5 in a minor complex, on the basis of a cross-peak to the major complex C3/C9 H5 proton. Given the separation of the G4 and G10 NH resonances (15 Hz), the lifetime of the major complex was estimated to be at least 40 ms.

Three T2/T8 H6 signals were assigned at 7.28, 7.32, and 7.42 ppm (Figure 7), from cross-peaks to T2/T8 CH_3 and to C3/C9 H5 signals. On the basis of cross-peak intensities, the first two were assigned to the minor complexes and the last one to the major complex. Chemical shift changes of actD ring protons and [d(ATCGAT)]$_2$ base protons of the major complex, compared with free drug and hexamer, are plotted in Figure 8, together with the same chemical shift changes for the actD–[d(ATGCAT)]$_2$ complex. Large upfield changes of 8H, 7H, and 6-CH_3 in both cases (Figure 8, I) are consistent with actD ring intercalating into DNA base pairs in these two complexes. The aromatic proton chemical shift changes of the two hexamers (Figure 8, II) also displayed a similar pattern.

It is noted that C3 NH_2 and C9 NH_2 protons all had downfield chemical shift changes upon complex formation (see Table I). This implies that the actD chromophore ring is sandwiched between G4 and G10 base rings in such a way the C3/C9 NH_2 protons are in a region experiencing a downfield ring-current shift effected by the actD chromophore.

Actinomycin D Conformation. The following intramolecular actD NOE contacts were detected, which are consistent with Sobel and Jain's (Sobell & Jain, 1972; Jain & Sobell, 1972) drug structure: 8H–Thrγ, Thrβ–DValγ (strong), Thrα–DValγ, Proα–Valα (strong), Proα–Valγ, and Proα–NMV NCH_3.

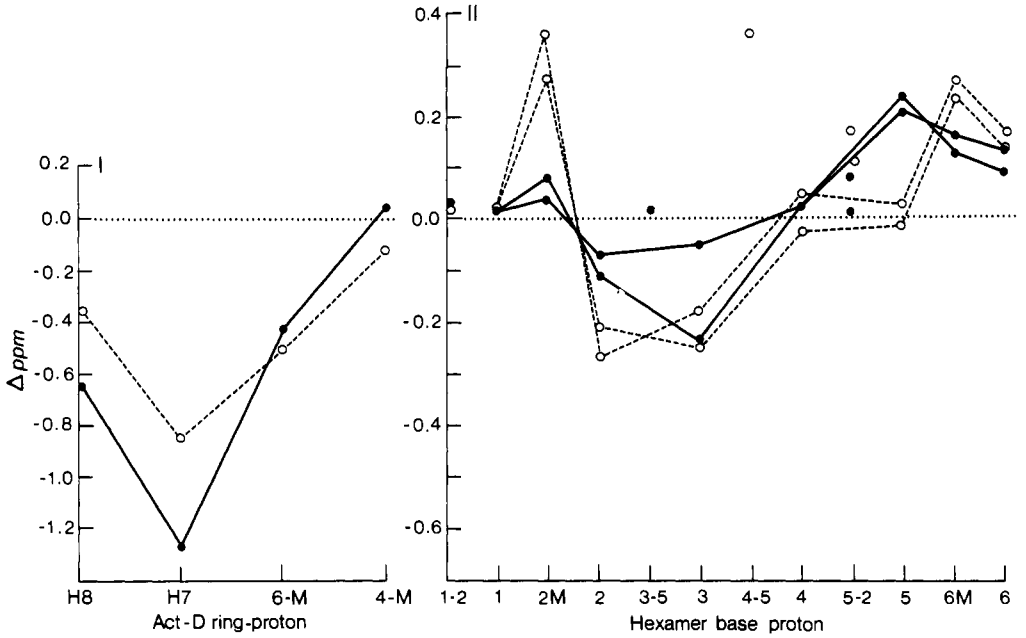

FIGURE 8: Chemical shift changes of actD chromophore ring protons (I) and oligonucleotide base protons (II) of actD–$[d(ATCGAT)]_2$ (solid circle and solid line) and actD–$[d(ATGCAT)]_2$ (open circle and broken line) compared to protons of free actD and DNA, respectively. The chemical shifts of actD–[d(ATGCAT)] and free actD–$[d(ATGCAT)]_2$ were from Brown et al. (1984). In part II, the purine H8 and pyrimidine H6 protons are indicated by appropriate residue numbers 1–6, while adenine H2, thymine methyl, and cytosine H5 protons are indicated by a second symbol, 2, M, or 5, after the residue number. Here the base protons on the two strands of DNA are named under the same convention and drawn as two lines. A H2 and C H5 protons are not included in the lines.

These results indicate that the conformation of actD in the major complex is similar to that observed in the crystalline complex with deoxyguanosine.

In the 2:1 actD–$[d(ATCGAT)]_2$ sample, an NOE cross-peak between actD peptide side-chain protons Thrγ and NMV NCH_3 was detected, while it was not detected in the 1:1 sample. Because of the distance between these protons in one actD molecule, this interaction must involve two different drug molecules. This suggests that in the 2:1 complex the peptide side chains of the two actD molecules overlap and both are located in minor groove of $[d(ATCGAT)]_2$. Also, the NMV α proton in the 2:1 complex appeared at a much lower field position, 3.32 ppm, compared to 2.94 ppm in the 1:1 actD–$[d(ATCGAT)]_2$ sample. At the higher drug:duplex ratio, the 2:1 complex is more predominant, as expected.

Intercalation Sites. Several internucleotide intrastrand NOE contacts at TC and GA steps were observed for the major complex in the 1:1 sample. Cross-peaks from other complexes were generally poorly resolved, but one internucleotide NOE peak was observed between protons at the CG step; no internucleotide NOE peaks between TC or GA steps were observed. These results are consistent with a central CG intercalated actD ring in the major complex and an off-center intercalated chromophore in the minor complex(es). The NOE cross-peaks are as follows: for the major complex, NOE peaks C3 H6–T2 H2″, C3 H6–T2 H2′, C3/C9 H5–T2 CH_3, C3/C9 H5–T2/T8 H6, and G4 H1′–A5 H8 were observed. Some of these NOE peaks were also detected in the 2:1 sample, indicating that the central intercalating complex still exists at that stoichiometry.

In addition to the major complex G4/G10 H8 proton at 7.93 ppm, another signal was identified at 7.84 ppm. This signal most likely belongs to the G4/G10 H8 proton of another complex. From this 7.84 ppm peak, another set of G4/G10 H2″, H2′, and H3′ signals can be identified through intraresidue NOEs at 2.48, 2.33, and 4.63 ppm, respectively (Figure 7). These resonances have lower intensities than the major complex signals. NOE peaks between the H3′ and H2′,2″ protons were also identified. One more G H3′ resonance can be located at 4.98 ppm, which connects with G H2′,2″ through NOE cross-peaks. Below 20 °C, the G H8 signal at 7.84 ppm was resolved into two peaks of approximately equal intensity. A weak NOE peak was observed between this G H8 and the C H2′ proton at 2.17 ppm (Figure 7). These additional G H8 signals can be explained by an actD–hexamer complex with the drug intercalated off center at the GA position. One set of off-center complex H2′,H2″ chemical shifts was quite different from those in the major complex, but the other set was similar. They most likely belong to G4 and G10, with one being adjacent to the intercalating drug chromophore, the other far away. Clear exchange peaks were detected between the two G H8 peaks and the two G H3′ peaks in the off-center complex.

NOE contact between major G4/G10 NH and T2/T8 NH signals was observed in the 1:1 sample (Figure 3, see Hexamer Imino and Amino Protons). This is additional evidence for a centrally intercalated major complex since the creation of an intercalation site at GA would increase the distance between imino protons so that a cross-peak would no longer be detectable by NOE measurements.

A number of NOE cross-peaks between major complex hexamer C3/C9 and G4/G10 protons and actD chromophore protons was detected. They include C3/C9 H5–actD 4-CH_3, C3/C9 H5–actD 6-CH_3, C3 H6–actD 6-CH_3 (Figure 7), and G4/G10 H1′–actD H8. These are evidence for actD chromophore intercalating adjacent to a G–C base pair in the hexamer but do not distinguish whether the drug ring is on the 3′ or 5′ side of the G residue.

Other 2D NOE peaks arising from $[d(ATCGAT)]_2$ and actD interactions were also identified from the 1:1 sample at 15 °C. The A5/A11 H2 signals (7.99, 7.93 ppm) gave relatively strong NOE peaks to the actD NMV NCH_3 (2.97

ppm) signal (Figure 7). The proximity of these protons can only be realized when the actD chromophore is between the central G–C base pairs. A similar contact was seen in our earlier study of actD intercalated between the two G–C base pairs of $[d(ATGCAT)]_2$ (Brown et al., 1984). The A1/A7 H2 signal at 7.85 ppm gave a weaker NOE peak to NMV NCH_3 that is further decreased in intensity at 20 °C. This behavior suggests that it comes from a minor complex. The proximity of A1/A7 H2 to NMV CH_3 protons can be explained with the actD ring system intercalated at the GA site in this complex. This A1/A7 H2 to NMV NCH_3 NOE cross-peak was observed with increased intensity in the 2:1 complex.

Two NOE cross-peaks between major A5/A11 H1′ signals (6.18, 6.28 ppm, assigned from hexamer intraresidue NOEs) and the NMV γ signal (0.82 ppm) were observed. These are consistent with the actD ring situated at the CG step, but not with a GA intercalated complex.

The C3/C9 H5 protons from the major and minor complex resonate at 5.61 ppm, while those from the minor complex are observed at 5.88 ppm. There are two relatively strong NOE contacts between a proton resonating at 5.61 ppm and the 6-CH_3 and 4-CH_3 of actD as well as a weak NOE contact with the T2/T8 CH_3 signal. These contacts are consistent with intercalation of the actD chromophore at the central CG site in the major complex. Another NOE peak was found between the minor C3/C9 H5 (5.88 ppm) and minor T2/T8 H6 (7.42 ppm) signals, suggesting placement of the drug ring at one GA site, but this T2/T8 H6 signal overlaps with one of the major C H6 signals; therefore, this evidence is ambiguous.

An NOE peak between the major G4/G10 NH and NMV NCH_3 resonances was detected. The proximity of these protons is consistent with an actD centrally intercalating complex. Since, in a GA intercalated complex the NMV NCH_3 from one of the peptide chains will still be close to one of the G NH protons and there is only one NMV NCH_3 signal detected, this NOE peak does not distinguish between center and off-center intercalation. The A1/A7 and T6/T12 hexamer protons in the complex were characterized by stronger intranucleotide NOE cross-peaks compared to protons in the rest of the hexamer, but no NOE contacts to actD chromophore protons were detected from them, indicating these AT sites were not close to the drug binding site.

Possible Modes of Binding. On the basis of the evidence presented above from optical and NMR experiments, we can infer that actD binds to $[d(ATCGAT)]_2$ at several sites via intercalation from the minor groove. There are several possible intercalation sites on the hexamer, the most probable of which are the central CG site and the off-central GA site, as suggested by the observed intermolecular NOEs. Binding to the former results in only one distinguishable complex regardless of the orientation of the chromophore. However, binding on the latter site results in two different complexes, depending on the orientation of the chromophore relative to the DNA bases. So there are three possible complexes involving binding of a single drug molecule. Similarly, there are three possible complexes with two bound drugs per duplex, assuming that two-drug complexes involve intercalation only at the off-central GA site. These binding modes are illustrated in Scheme I.

Scheme I: Types of Complexes Formed by Actinomycin D with $d(ATCGAT)_2$

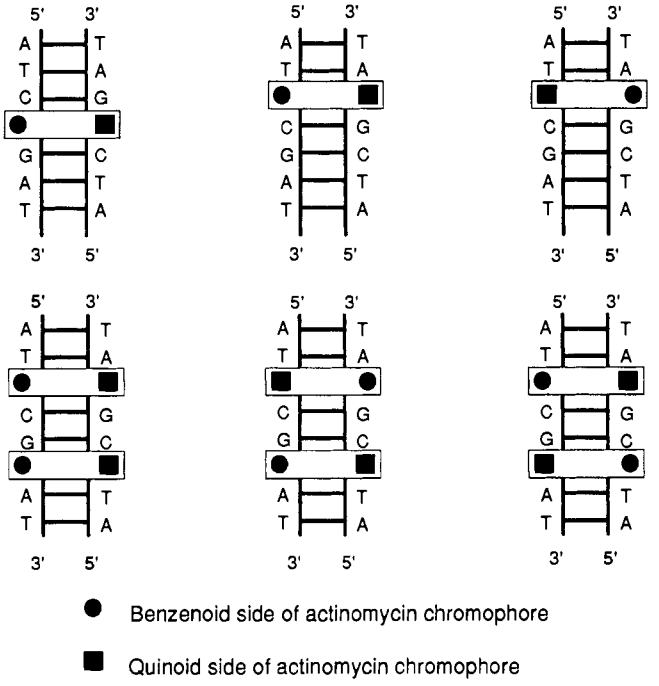

(*a*) *Imino Proton Spectra.* The imino proton spectra at all but perhaps the highest drug:duplex ratio show three peaks attributable to G NH imino protons. In samples at low actD:duplex ratios, one expects that the one-drug complexes will predominate, of which three are possible. The actD molecule is almost symmetric and, because of this, most of the imino proton peaks do not show splitting. The G NH protons at 12.10 ppm provide the one exception in that they have actually been resolved into two peaks of almost equal intensity (see Figure 4) and assigned to the CG intercalated complex. This leaves peaks at 12.75 and 12.45 ppm, which may represent either one or two other complexes. Since the peak at 12.45 appears to decrease in relative amplitude while the peak at 12.75 increases in amplitude as the drug:duplex ratio is increased from 1:1 to 3:1, these two peaks probably arise from two different complexes. This is in accord with the data on nonexchangeable protons, where there is clearer evidence for the presence of three complexes, one major complex and two minor ones at a stoichiometry of 1:1. At higher drug:duplex ratios, the peak at 12.75 ppm appears quite substantial, while that at 12.45 ppm diminishes in significance. Because of the potentially different solvent-exchange properties for various G NH protons, it is not feasible to use the observed amplitudes as a measure of the relative populations of the complexes. This is done more reliably by using resonances of the nonexchangeable protons.

In terms of T2/T8 protons, at high drug:duplex ratios, there is one strong signal, near the position of the internal T NH proton in the free duplex, and one very weak, broad signal at higher field. The strong resonance furthest downfield appears to show some evidence of splitting, most convincingly at lower drug:duplex ratios. It is difficult to assess whether this splitting represents two different complexes with magnetically equivalent T NH protons or one complex with magnetically nonequivalent protons. Due to its position and the NOEs produced to the G NH protons at 12.10 ppm (see Figure 6), this peak is assigned to the T2/T8 NH protons associated with the major complex. The lack of any other strong T NH resonance at higher drug:duplex ratios suggests that in the 2:1 noncentrally intercalated complex the internal T NH proton is destabilized with respect to exchange. This could well be due to the extensive conformational changes required to accommodate two bound drug molecules separated by only two base pairs.

This leaves the peak at 12.45 ppm to be assigned. It most likely arises from an off-center-intercalated complex containing only a single bound drug molecule. It appears to be much

smaller in magnitude than the other upfield peaks, but this may be due to solvent-exchange properties as well as population differences. More significantly, as the drug:duplex ratio increases from 1 to 3, the intensity of this resonance decreases substantially. This peak may come from either one or both of the possible off-center, single-drug complexes.

(*b*) *Nonexchangeable Protons*. The H8 proton of the actD chromophore has been observed in the 1:1 drug–duplex sample from three different complexes, the major complex and two other complexes. The two minor complexes may consist of single-drug complexes or both single- and double-drug complexes. These two minor species, then, represent the two forms of off-center-intercalated complexes. Parallel to these results on the actD H8 proton, two sets of signals, in addition to the major one, were observed for the guanosine H8 and sugar protons. Unfortunately, resolution was limited in the nonexchangeable proton spectrum in the samples containing the 2:1 and 3:1 drug:duplex ratios, so a detailed analysis was not possible.

Conclusions

The optical and NMR data presented above indicate that actD binds to $[d(ATCGAT)]_2$ by intercalation in aqueous solution. The absence of the drug's preferred binding sequence, GC, in this hexamer results in several different bound complexes whose relative populations depend on the drug:duplex ratio and temperature. For each of the bound complexes, evidence based on circular dichroism spectra and intra- and intermolecular NOEs was obtained for an intercalative mechanism of binding, with the peptide groups of the drug positioned in the minor groove. At high drug:duplex ratios, there was evidence of a 2:1 actD–$[d(ATCGAT)]_2$ complex involving off-center intercalation. At these higher drug:duplex ratios, however, the data implied that the single bound drug complex with actD intercalated at the central CG site was still present in substantial proportions. This suggests that the centrally intercalated complex has a strong binding affinity relative to the off-center complexes. The imino proton spectra at low drug:duplex ratios also support this observation.

Recent studies (Scott et al., 1988) have shown that two actinomycin molecules can bind to the sequence GCGC by intercalation at the GC sites, with only two base pairs separating the bound chromophores, without any significant binding to the central CG site. In our studies described above, we have also found evidence for two bound ligands separated by only two base pairs. A major difference between the results of Scott et al. (1988) and our results is that we observe a mixture of several bound complexes, even at high drug:duplex ratios. This makes it difficult to obtain a very high resolution picture of the complexes formed, but indicates that the relative affinities of actD for CG and GA sites are not markedly different, although the former appears to be the stronger binding site. The reasons for this difference may lie in the difference in DNA conformation at alternating and nonalternating pyrimidine–purine sequences or in the difference in base composition. Additional studies will be necessary to evaluate these possibilities.

Acknowledgments

We acknowledge the use of the spectropolarimeter in Professor J. T. Yang's laboratory in the Biochemistry and Biophysics Department, UCSF. We thank Dr. Corey Levenson, Dragan Spasic, and Lauri Goda of Cetus Corp., Emeryville, CA, for providing the $[d(ATGCAT)]_2$ sample. We also thank Dr. Max Keniry for helpful discussions and Elma P. Belenson for expert typing of the manuscript.

Registry No. actD–$[(ATCGAT)]_2$ complex (1:1 ratio), 120496-93-7; actD–$[d(AT)_5]_2$ complex, 120544-87-8; actD–$[d(ATGCAT)]_2$ complex, 53360-01-3; $[d(ATCGAT)]_2$:actD complex (1:2 ratio), 120523-75-3.

References

Allen, F. S., Moen, R. P., & Hollstein, U. (1976) *J. Am. Chem. Soc. 98*, 864–865.

Allen, F. S., Jones, M. B., & Hollstein, U. (1977) *Biophys. J. 20*, 69–78.

Boelens, R., Scheek, R. M., Dijkstra, K., & Kaptein, R. (1985) *J. Magn. Reson. 62*, 378–386.

Brown, S. C., Mullis, K., Levenson, C., & Shafer, R. H. (1984) *Biochemistry 23*, 403–408.

Chen, F.-M. (1988) *Biochemistry 27*, 1843–1848.

Davis, D. G., & Bax, A. (1985) *J. Am. Chem. Soc. 107*, 2820–2821.

Hore, P. J. (1983) *J. Magn. Reson. 54*, 539–542.

Jain, S. C., & Sobell, H. M. (1972) *J. Mol. Biol. 68*, 1–20.

Krugh, T. R. (1972) *Proc. Natl. Acad. Sci. U.S.A. 69*, 1911–1914.

Lybrand, T. P., Brown, S. C., Creighton, S. C., Shafer, R. H., & Kollman, P. A. (1986) *J. Mol. Biol. 191*, 495–507.

Müller, W., & Crothers, D. M. (1968) *J. Mol. Biol. 35*, 251–290.

Narang, S. A., Brousseau, R., Hsiung, H. M., & Michniewicz, J (1980) *Methods Enzymol. 65*, 610–620.

Reid, D. G., Salisbury, S. A., & Williams, D. H. (1983) *Biochemistry 22*, 1377–1385.

Remers, W. A. (1978) in *The Chemistry of Antitumor Antibiotics*, Vol. 1, Wiley, New York.

Schara, R., & Müller, W. (1972) *Eur. J. Biochem. 29*, 210–216.

Scott, E. V., Jones, R. L., Banville, D. L., Zon, G., Marzilli, L. G., & Wilson, W. D. (1988) *Biochemistry 27*, 915–923.

Sobell, H. M. (1973) *Prog. Nucleic Acid Res. Mol. Biol. 13*, 153–190.

Sobell, H. M., & Jain, S. C. (1972) *J. Mol. Biol. 68*, 21–34.

Waring, M. (1981) in *The Molecular Basis of Antibiotic Action* (Gale, F., et al., Eds.) pp 314–333, Wiley, London.

Wells, R. D., & Larson, J. E. (1970) *J. Mol. Biol. 49*, 319–342.

Wilson, W. D., Jones, R. L., Zon, G., Scott, E. V., Banville, D. L., & Marzilli, L. G. (1986) *J. Am. Chem. Soc. 108*, 7113–7114.